The impact of capacitor coupled sub-station in rural electrification of sub-Saharan Africa

Michael Juma Saulo[1, *], Charles Trevor Gaunt[2]

[1]Electrical Department, Technical University of Mombasa, Mombasa, Kenya
[2]Electrical Department, University of Cape Town, Cape Town, South Africa

Email address:
michaelsaulo@yahoo.com (M. J. Saulo), ctgaunt@uct.ac.ke (C. T. Gaunt)

Abstract: The overall electricity access rate is still very low in most sub-Saharan African (SSA) countries. The rate is even lower in rural areas where most of the population in these countries lives. One of the main obstacles to rural electrification (RE) is the high cost of laying the distribution infrastructure owing to the dispersed nature of loads and low demand. Thus, electrifying the rural areas needs to be considered holistically and not just on the financial viability. To reduce cost, it is important that un-conventional rural electrification (URE) technologies, which are cheaper than the conventional ones be explored. This paper investigates the adoptability and maximum penetration level of sub-station based URE i.e. Capacitor Coupled Sub-station (CCS) technologies in power transmission networks with regard to voltage quality, stability, and capacity constraints without steady and transient state voltage violation. Quantitative data collected from practical power transmission lines in Kenya were used for empirical and analytical approaches developed in this research. The paper developed a method of determining maximum allowable penetration level of CCS without steady state voltage violation derived from a modified distributed generation analogy. The method was based on determination of voltage sensitivities from linearized power system model. Consequently, this method was used to validate repetitive power flow simulations carried out in the case studies.

Keywords: Capacitor Coupled Sub-Station, Un-Conventional Rural Electrification, Distributed Generation,
Penetration Level

1. Introduction

In most SSA rural areas, the concentration of electricity users is low and cost of deploying a conventional sub-station is prohibitive. As a result, in many cases power utilities will not be able to generate an adequate return on the large investment necessary to bring a conventional distribution sub-station on line. Conversely, there are large numbers of rural communities in these areas living around or in close proximity to high voltage transmissions lines but are un-electrified. The main obstacle is that these lines are carrying high voltages that cannot be directly and cheaply used for electrification. Therefore, in order to address the drawbacks associated with prohibitive costs of conventional

sub-stations, URE sub-station are explored in this paper [1]. The focus of this paper is based on the un-conventional sub-station technology known as; Capacitor Coupled Sub-station (CCS) that taps directly into the transmission overhead lines. Figure 1(a), shows a single line diagram of the CCS sub-station technology. Where; C_1 and C_2 are the divider capacitors, L is the inductor added in series to cancel the Thévenin reactance that is; $C_{th} = C_1 + C_2$ at 50Hz, FSC is the Ferro-resonance Suppression Circuit and Tx is the fixed turns ratio isolating transformer connected to the load. Whereas, Figure 1(b), is the pictorial diagrams for CCS system.
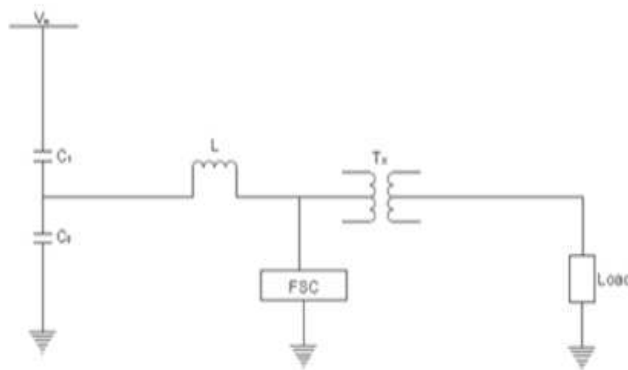
Figure 1. (a) and (b) Single line and pictorial diagram of a CCS

This URE sub-station technology offer major opportunities for reduction of construction, operating and maintenance costs of grid-based rural electrification in sub-Saharan Africa (SSA). In many cases, careful attention to system design enables construction cost to be reduced by up to 30%, contributing significantly to the pace, scope and affordability of the rural electrification services [2]. Grid-based electricity offers a cheaper option for lighting and small appliances usage in rural settlements in SSA. Therefore, there is no need to apply the design standards used for more heavily loaded urban systems when designing rural electrification networks. The rural distribution system can be designed for actual loads, often not more than a few kilowatt-hours per month, imposed to it by rural households [3]. Although consumptions grow, this is usually at a slow pace and provided necessary design provisions are made, systems can be upgraded relatively cheaply later. Therefore, careful and empirical analysis of URE system design and implementation practices has great potential for significant cost savings, which can improve affordable access of electricity to rural consumers, contributing to sustainability of electricity services in rural areas.Rural electrification has two primary objectives. First, to improve the economic status of the rural population by increasing the productivity of human and labour and secondly, to promote rural welfare by providing an environment equal in comfort and convenience to that enjoyed in urban areas [4]. This paper investigated the adoptability and maximum penetration level of sub-station based URE i.e. Capacitor Coupled Sub-station (CCS) technologies in power transmission networks with regard to voltage quality, stability, and capacity constraints without steady and transient state voltage violation.

1.1. Conventional Vs. Un-conventional Rural Electrification

A World Bank report [2000] recommended, "There is a need to break out from the traditional conventional mould, to review specific needs of rural community, to go back to basic principles, and to develop designs that most cost-effectively address their needs." Surprisingly, these calls have remained largely ignored, especially in SSA. These are evidenced by the common centralized generation with high voltage transmission to regional sub-stations. Consumers are then supplied using lower voltage lines reducing the voltage closer to the customers [5]. Quite often rural networks are over-designed, since there is a perception that under design carries more risk for organizations than the over-design because the former provide criticism in the future. Therefore, designers of URE based technologies need to take advantage of already existing built-in extra infrastructure capacity, especially where there is an extensive system in place when designing the URE projects. Most transmission networks in SSA were built more than 50 years ago during the colonial era. These lines on their path from power source to major urban centers typically transverse many un-electrified rural areas. In recent times these areas have developed and their need for electrical energy has actually doubled if not tripled. Consequently, there is dire need to approach rural electrification planning and design from un-conventional perspective. In other words planning following existing developments [6]. In this paper, URE technologies concept are taken to mean "the rural electrification technologies which do not follow traditional methods" for example, three phase distribution system with three or four wires, conventional vertical transmission and distribution approach and conventional bulky transformer sub-stations among others.

2. Modeling of Capacitor Coupled Sub-Stations

The design of a voltage divider which forms the CCS system includes several steps in steady state considerations and transient state analysis. The subsequent section discusses these designs from two perspectives i.e. (i) modeling CCS without transmission line (ii) modeling CCS on a transmission line. The later sections also consider the CCS placement on a transmission line before finally coming up

with the practical design of the CCS parameters.

2.1. Modeling CCS without Transmission Line

The purpose of a CCS is to reduce the high voltage of a transmission line to a distribution voltage level. For this reason, the system is usually referred as a capacitive transformer. Figure 2, illustrates the operating principle of the capacitor divider considering a phase to ground connection [7, 8, 9].
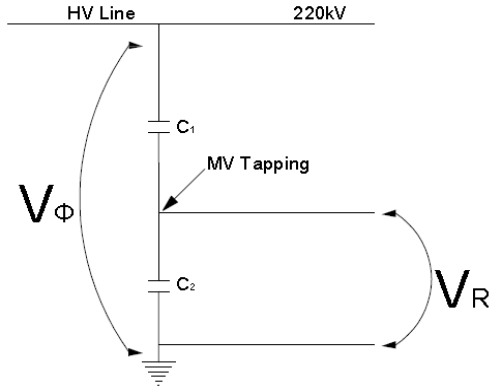

Figure 2. *Capacitive voltage divider connected phase- to- ground*

Let $V_\emptyset$ and V_R be the transmission line and the reduced voltage respectively then the voltage ratio as a function of the divider impedances (Z_1 and Z_2) or capacitance C_1 and C_2 is:

$$V_R = \frac{Z_2}{Z_1 + Z_2} V_\varphi = \frac{C_1}{C_1 + C_2} V_\varphi \qquad (1)$$

The coefficient $Z_1/(Z_1+Z_2)$ is the transformation ratio of the system. The impedance of the Thévenin circuit from Figure 3 is very high and causes poor voltage regulation with big loads. The choice of capacitor C_1 and C_2 must satisfy two conditions. The first one is the voltage across bank C_2 for a no load condition corresponds to the selected distribution voltage V_R. This condition can be defined by equation 2 in the form of;

$$\frac{Z_1}{Z_2} = \frac{V_\varphi}{V_R} - 1 \qquad (2)$$

The second condition to be satisfied is that the maximum steady state voltage V_{max} across each capacitor unit must be less than or equal to its normal voltage V_n. This condition can be stated for bank C_1 for the most critical situation which is a full resistive load and it is expressed by the following inequality [9].

$$V_{C1(max)} \leq V_{nC2} \qquad (3)$$

Where;

$$V_{C1(max)} = \sqrt{(I_L Z_L)^2 + (V_\phi - V_R)^2}$$

$$V_{nC2} = \sqrt{P_{nC2} Z_2}$$

I_L = Maximum current through the load
P_{nc1} = Nominal power of bank C_1
Z_L = Impedance of an inductor connected in series with load.

On the other hand, the worst case for bank C_2 is a full inductive load. Assuming that the lowest power factor that can be encountered is 0.8, and then the following inequalities can be expressed as follows [9]:

$$V_{C1max} = \sqrt{(0.8 I_L Z_L)^2 + (V_R + 0.6 I_L Z_L)^2}$$

$$\leq V_{nC1} = \sqrt{P_{nC2} Z_2} \qquad (4)$$

Given that:

$$Z_L = \frac{Z_1 Z_2}{Z_1 + Z_2} \qquad (5)$$

Where: P_{nC2} = nominal power of bank C_2

By substituting Z_L in both inequalities 3 and 4, two quadratic inequalities are obtained, having Z_1 and Z_2 as variables as expressed below:

$$Z_1^2 \left(\frac{I_L}{1 + \dfrac{Z_1}{Z_2}} \right)^2 - Z_1 P_{nC2} + (V_\Phi - V_R)^2 \leq 0 \qquad (6)$$

$$Z_2^2 \left(\frac{I_L}{1 + \dfrac{Z_1}{Z_2}} \right)^2 - Z_2 \left(P_{nC2} - 1.2 \frac{I_L V_R}{1 + \dfrac{Z_2}{Z_1}} \right) + V_R^2 \leq 0 \qquad (7)$$

By choosing the nominal power P_n of each bank the inequalities 6 and 7 yield intervals of feasible values for C_1 and C_2. The interval for C_2 can be converted into the interval for C_1 when multiplied by the constant ratio Z_1/Z_2. The intersection of this interval with the one obtained from P_{nC1} yields a range of feasible values of C_1, and the corresponding range of C_2 for the previously selected powers P_{nC1} and P_{nC2}.

This technique can be directly applied when all the units of the banks are identical. This involves an iterative process in which the nominal powers are increased until the feasible intervals allow a selection of single phase units that best approximate the impedance ratio in equation 2.

If the capacitors units are of different voltage class or power rating, the nominal voltage V_n of the bank may be obtained as follows: First define the nominal current of each unit "j".

$$I_{nj} = \frac{P_{nj}}{V_{nj}} \qquad (8)$$

Then determine the minimum current $I_{n\ min}$ found and multiply it by the summation of their impedances:

$$V_n = I_{n(min)}\left(\sum_j \frac{V_{nj}^2}{P_{nj}}\right) \quad (9)$$

By following this procedure the capacitor units of the prototype systems may be chosen.

2.2. Modeling CCS on Transmission Line

Figure 3, shows the schematic representation of CCS connected to the transmission line. An equivalent circuit is shown in Figure 4 where k is a factor between zero and one [10].
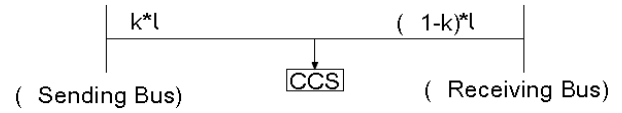

Figure 3. Schematic representations

This factor defines the location of CCS along the length of the transmission line and l is the length of the transmission line. The transmission line parameters are obtained using factor k. Variable with subscript 'a' refers to the first portion of the line whose length equals k*l while subscript 'b' refers to the last portion of the line. Length of this portion is equalto (1-k)*l.
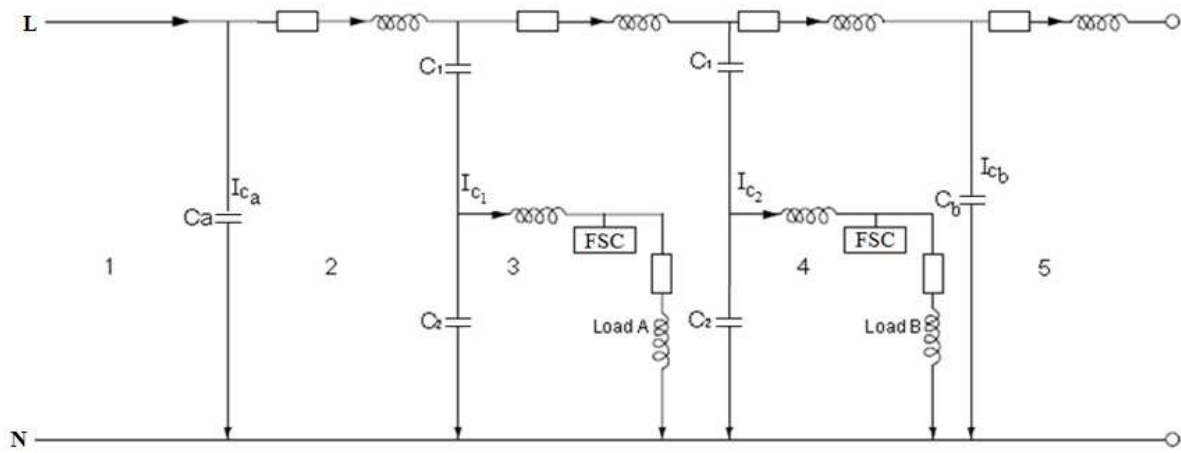

Figure 4. Systems equivalent circuit [9]

2.2.1. Steady State Modeling

Steady state equations have been derived [10] from the models shown in Figure 4 the equations relate to the receiving and sending end voltage and current of the transmission line including the load terminal of the CCS unit.

$$V_R = \left[\frac{2}{(1+j\omega C_b Z_b)}\right]\left[\frac{V_d}{C_{12}}+\frac{I_d Z_a}{C_{12}}-\frac{V_s}{2}(1+j\omega C_a Z_a)+\frac{I_s Z_a}{2}(2+j\omega C_a Z_a)-\frac{I_R Z_b}{2}(2+j\omega C_b Z_b)\right] \quad (10)$$

$$I_R = \left[\frac{1}{(1+j\omega C_b Z_b)}\right][I_s(1+j\omega C_a Z_a)-j\omega C_b V_R + j\omega C_2 V_d - j\omega C_a V_s - I_d(1-j\omega C_2] \quad (11)$$

2.2.2. Transient Modeling

The equivalent circuit used for modeling is the one in Figure 4. The circuit has been divided into five loops. Equations derived are shown below;

$$R_a\frac{di_1}{dt}+L_a\frac{d^2i_1}{dt^2}+\frac{1}{C_a}(i_1-i_2)=\frac{dV_s(t)}{dt} \quad (12)$$

$$\frac{1}{C_a}(i_2-i_1)+R_a\frac{di_2}{dt}+L_a\frac{d^2i_2}{dt^2}+\frac{1}{C_1}(i_2-i_4)+\frac{1}{C_2}(i_2-i_3)=0 \quad (13)$$

$$\frac{1}{C_1}(i_3-i_2)+R\frac{di_3}{dt}(i_3-i_4)+L\frac{d^2i_3}{dt^2}+(i_3-i_4)+\frac{dV_d(t)}{dt}=0 \quad (14)$$

$$\frac{1}{C_1}(i_4 - i_2) + R_b\frac{di_4}{dt} + L_b\frac{d^2i_4}{dt^2} + \frac{1}{C_b}(i_4 - i_5) - \frac{dV_d(t)}{dt} + L\frac{d^2i_4}{dt^2}(i_4 - i_3) + R\frac{di_4}{dt}(i_4 - i_3) = 0 \qquad (15)$$

$$R_b\frac{di_5}{dt} + L_b\frac{d^2i_5}{dt^2} + \frac{dV_R}{dt} + \frac{1}{C_b}(i_s - i_4) = 0 \qquad (16)$$

These equations may be used to show the variation of load voltage with load power. The idea is to find an optimum operating load that can be supported before the voltage begins to collapse. The load tests are done at variable load power factor. The load model used is that of a series R-L.The system is tested at different level of demand. Real power demand (P) may be fixed to a different value and reactive power demand (Q) varied to operate at different load power factor between 0.2 lagging and unity [10].

2.2.3. Modeling Practical Element of the CCS

Section 2.1 showed the theoretical design of a CCS unit at steady state condition. It is important to note that the capacitors used for the design of CCS have inherent equivalent series resistance (ESR). Hence, they experience losses based on ESR designed value.
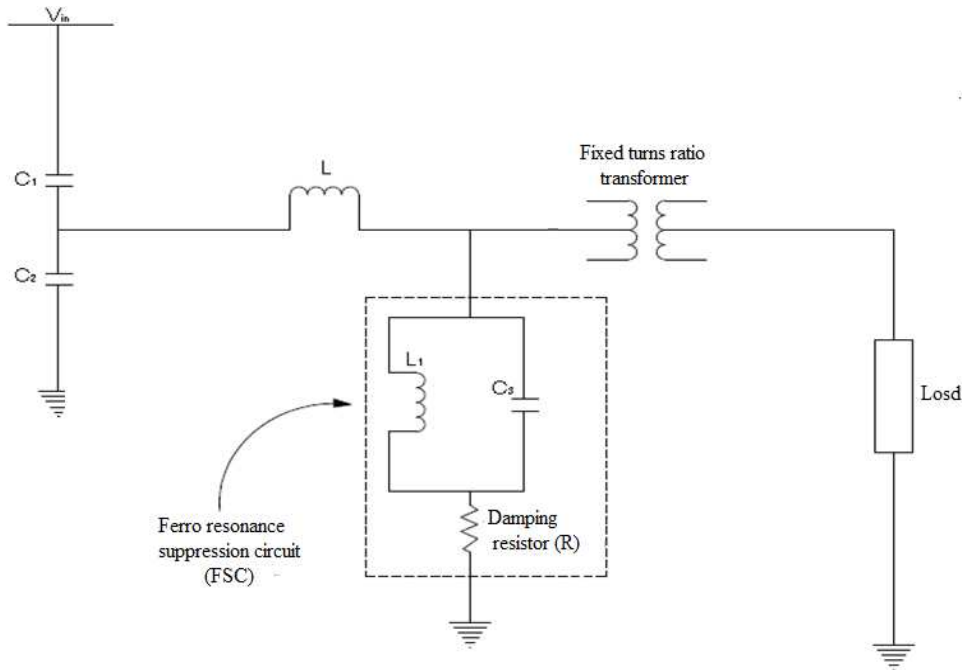

Figure 5. Capacitor Coupled Sub-station schematic diagram [7]

The practical approach to design is to ensure that the voltages V_{C1} and V_{C2} for capacitor C_1 and C_2 (see Figure 5) do not exceed nominal values under extreme steady state loading conditions. MATLAB Sim Power program is used to analyse transient behaviour for designs of low and high impedance obtained at steady state conditions. In order to determine the value of the capacitor we consider two boundary conditions namely:

- The heat dissipated should be such that the temperature rise should not exceed the maximum temperature rise of the capacitor based on its ESR designed value.
- The combination of the capacitors that make the capacitor divider circuit should result in the target output phase voltage which in this case is 33kV (Note: 33kV is the main distribution voltage used for rural electrification in Kenya).

According to [11], It can be shown by use of the charge conservation law, that heat dissipated by the capacitor divider circuit composed of C_1 and C_2 is given by;

$$\Delta E = \frac{C_1 C_2}{C_1 + C_2}\frac{(\Delta V)^2}{2} \qquad (17)$$

Where ΔE is the energy dissipated as heat and ΔV is the change in voltage.

In this case ΔV = (127-33) kV = 94kV, (Note: $220kV/\sqrt{3} = 127kV$)

Therefore;

$$\Delta E = \frac{C_1 C_2}{C_1 + C_2}\frac{(94\times1000)^2}{2} = \frac{C_1 C_2}{C_1 + C_2}\frac{94^2}{2}10^6 \qquad (18)$$

Equation 18 suggests that the capacitive equivalent has to be in the order of microfarads in order to keep losses as low as possible. The values of C_1 and C_2 are arrived at by use of iterative method.

Capacitors are chosen in such a way that C_1 is smaller than C_2 by a factor that can give the desired voltage level at the output.

Therefore, considering the desired voltage of ± 6% of 33kV and using equation 1, the capacitor voltages were chosen as follows; $C_1 = 0.5\ \mu F$ and $C_2 = 1.5 \mu F$.

This can be demonstrated by the calculation shown below, where; $V_\varnothing$ is the transmission line voltage per phase and V_R is the reduced or output voltage.

$$V_R = \frac{C_1 V_\varphi}{C_1 + C_2} = \frac{0.5 \times 127 \times 10^{-6} \times 10^3}{(0.5 + 1.5) \times 10^{-6}} = 31.75 kV$$

Thus, 31.75kV becomes our base voltage which is within ±6% of 33kV. From Figure 6, an inductor L is added to the capacitive voltage divider C_1 and C_2 to cancel the Thévenin impedance $C_{th} = C_1 + C_2 = C_f$ at 50Hz. The regulation is done by adjusting C_1, C_2 and L so that they satisfy $LC\omega^2 = 1$, where $\omega = 2\pi 50$. Therefore, the value of L is calculated as;

$$L = \frac{1}{C_f \omega^2} = \frac{1}{(0.5 + 1.5) \times 10^{-6} (314)^2} = 5.071 H$$

For designing the desired Ferro-resonance suppression circuit (FSC) the following points are considered: The capacitor C_3 is connected in parallel to the inductor L_1 and both are connected in series with a damping resistor R. Thus, $C_f = C_{th} = C_1 + C_2 = 0.5 + 1.5 = 2.0 \mu F$.

And $L_f \le \dfrac{1}{(2\pi f)^2 C_f}$, Therefore; $L_1 = L_f \le 5.071 H$.

The damping resistor R should be in the range of the system load. Figure 6 and 7 shows the peak power over the daily load profile load and average power demand curve respectively for a typical rural village in Kenya [12]

Figure 6 shows the peak power demand over the daily load profile. The peak load is considered at 391.40.kW. The average load requirement for these rural communities is taken as 30% (based on the diversity factor of the rural loads) of the peak power demand over the daily profile as shown in Figure 7. The average power demand was modeled with regards to the communities continuous rating load requirement. Based on these findings an average load of 100kVA at unity power factor was considered for the optimum design of the CCS unit(s). The design assumption was that, the tap-off voltage was at ±6% of 33kV then stepped down using the isolating transformer to 33kV /0.240kV for distribution purposes.
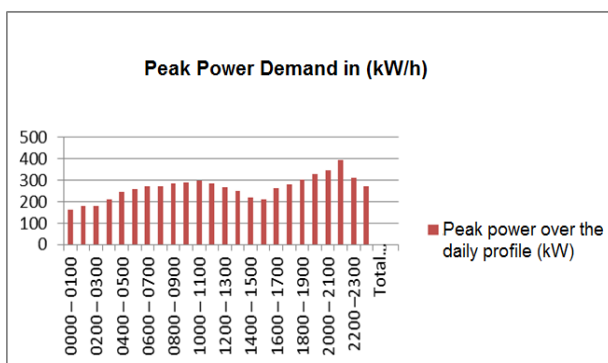
Peak Power Demand in (kW/h)

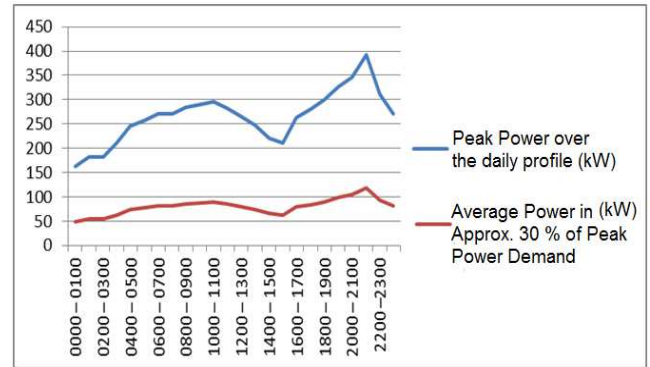*Figure 6. Peak power over the daily profile (kW)*

Figure 7. Average power demand curve for a typical rural village

3. CCS on Power Transmission Line (Case Study)

3.1. Simulation Scenarios

System energisation at no-load and load on/off were carried out. Simulations were first done with the line not loaded followed by a loaded line and finally the line under short circuit or transient conditions. Voltage and power variable constraints were taken into considerations. The CCS units were included at different distances. Simulations scenarios with different configurations of the system were carried out to investigate the transmission systems steady and transient state behaviour. The CCS units were subjected to the same loading conditions and ratings as follows;

- Actual Load of transmission line - 125MW.
- Transformer rating - 70kVA.
- CCS heavy Load – 100kW.
- CCS Light Load – 1kW.
- C_1 – Varying between 0.12 to 0.5 µF.
- C_2 –Varying between 0.4 to 1.5 µF
- L- Varying between 2.5 to 5.071H
- Occasionally switching on/off the 10MVAr reactor.

Different system configurations for simulations were classified as follows;

- Models with CCS and without FSC and load at steady and transient states
- Models without CCS for unloaded and loaded conditions
- Models with CCS and FSC for unloaded and loaded conditions
- CCS with FSC at different distances with line unloaded and loaded
- CCS with FSC models for transient stability cases.

For this paper the first two scenarios are presented as samples of the simulation carried out. Loadability analysis was also done to show the variation of the voltage profile with load power (MW) at different power factors. The steady state simulations focused and analyzed three main voltage points on the system, namely;

- Tap-off voltage (V_T), the point at which voltage is

tapped on the transmission line.

- Voltage divider (V_D), the voltage between the capacitor bank C_1 and C_2 or voltage at the capacitive divider point.
- Load terminal voltage (V_L) is the voltage at the load

point.

3.2. CCS Model without the FSC and Load at Steady State
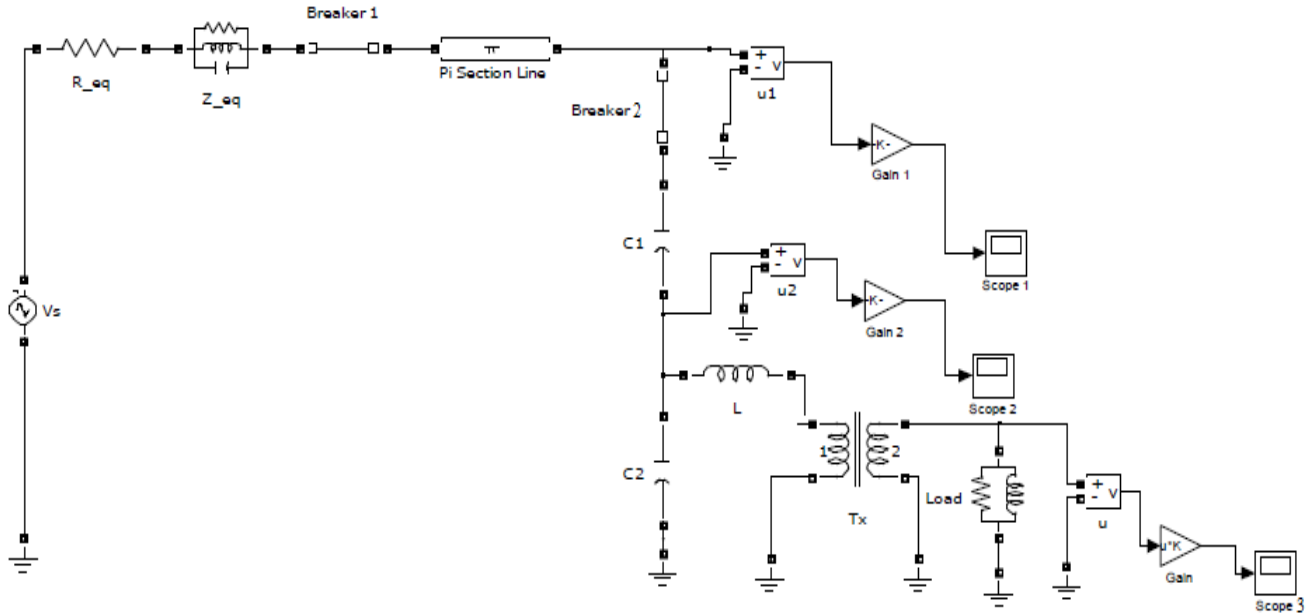

Figure 8. Model for the line with one CCS and without FSC

Figure 8, shows a sample model for the line with one CCS and without FSC used for steady state simulation scenario. Scope 1 measured the tap off voltage (V_T), while scope 2 measured voltage at the capacitive divider point (V_D) and scope 3 measured the load voltage (V_L). It is important to note that, the position of the CCS did not change the result for one CCS penetration. Similar results were obtained, when the simulation was carriedout using the same model with two and three CCS penetration respectively. For the purpose of this research the CCS were assumed to be located with uniform distance.

For model with one CCS penetration, each pi section represented 220km while with two CCS penetrations each pi section represented 147km. It was important to note that the value of C_1 C_2 and L used were derived from the values developed in section two. The values of C_1 C_2 and Lcould be varied to give different voltage measurements as long as the allowable voltage violation limit of 240V with ± 2.5% at the load terminal (V_L) was not surpassed for the low voltage side. However, for the high voltage side, that is the tap-off (V_T) and divider voltage (V_D), the allowable voltage violation was 6% of the nominal voltage. Theallowable tap-off voltage (V_T) and divider voltage (V_D) ranges between (119.38 to 134.62kV) and (31.02 to 34.98kV) respectively. While, the load terminal voltage (V_L) ranges between (0.234 to 0.246 kV). Five configurations of the models were considered during simulation, ranging from a single CCS penetration at the end terminal of the transmission line to five CCS penetrating the system. Different arrangements at specific distances on the transmission line were considered and measurements taken.

The CCS simulation. Results showed that the tap-off voltage (V_T) on the transmission line reduced as the number of CCS penetration increased. The tap-off voltage drop of the five CCS units connected on the transmission line conformed to the allowable voltage drop. Thus, no voltage compensation technique was required for the five CCS units penetration at steady state. This meant that the system was self-compensated for this scenario. Even though, at lower penetration of CCS units (i.e. 1 to 4 units), the voltage magnitude was slightly higher and above the acceptable range. Therefore, in such instance compensation was necessary. Interestingly, the divider voltage (V_D) and the tap-off voltage (V_T) seemed to be within the allowable voltage drop for all the five configurations. Although, for the same scenario load voltage (V_L) was below the acceptable value. In summary it was observed that penetration of five CCS units can be adopted for this scenario as long as a tap changing transformer is installed at the output of the system to mitigate the low voltage on the load side. Therefore, five CCS units penetration gave the most probable acceptable voltage profile for the steady state scenario with FSC and unloaded condition.

3.3. CCS Model without FSC at Transient State

Transient state means any sudden change in a circuit, as a result of disturbance. This may occur during switching (closing or opening of a circuit), short circuit or even saturation. In this case the transient state condition was simulated by the use of switching on/off a circuit breaker and injecting a disturbance signal. Figure 9, below shows the layout of the CCS system model used for simulating transient

conditions including monitoring instruments and disturbance (signal 1-4) injected. For this paper only Signal1 simulation samples are presented. The resulting transients after disturbance signal 1 injection are shown in Figure 10 (a-e) for signal 1 injection. The waveform measurements were displayed out as follows;

Scope 1 measured the tap off voltage (V_T)
Scope 2 measured the divider voltage (V_D)
Scope 3 measured the system current

Scope 4 measured the load current
Scope 5 measured the load voltage (V_L)

It is important to note that, all the graphs in this section are labeled in the following manner. Graph (c) and (d) waveforms represent graphs of current against time in (seconds) and graphs (a), and (e) waveforms are graphs of per unit kilovolt (kV) against time (seconds). Graph (b) waveform is a graph of kilovolt (kV) against time (seconds)
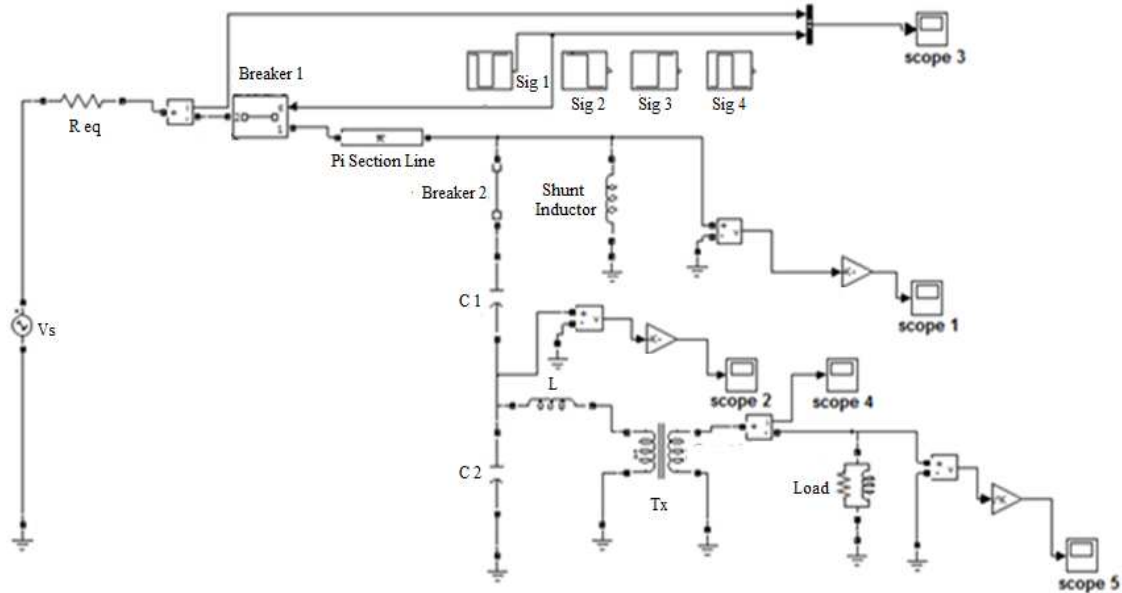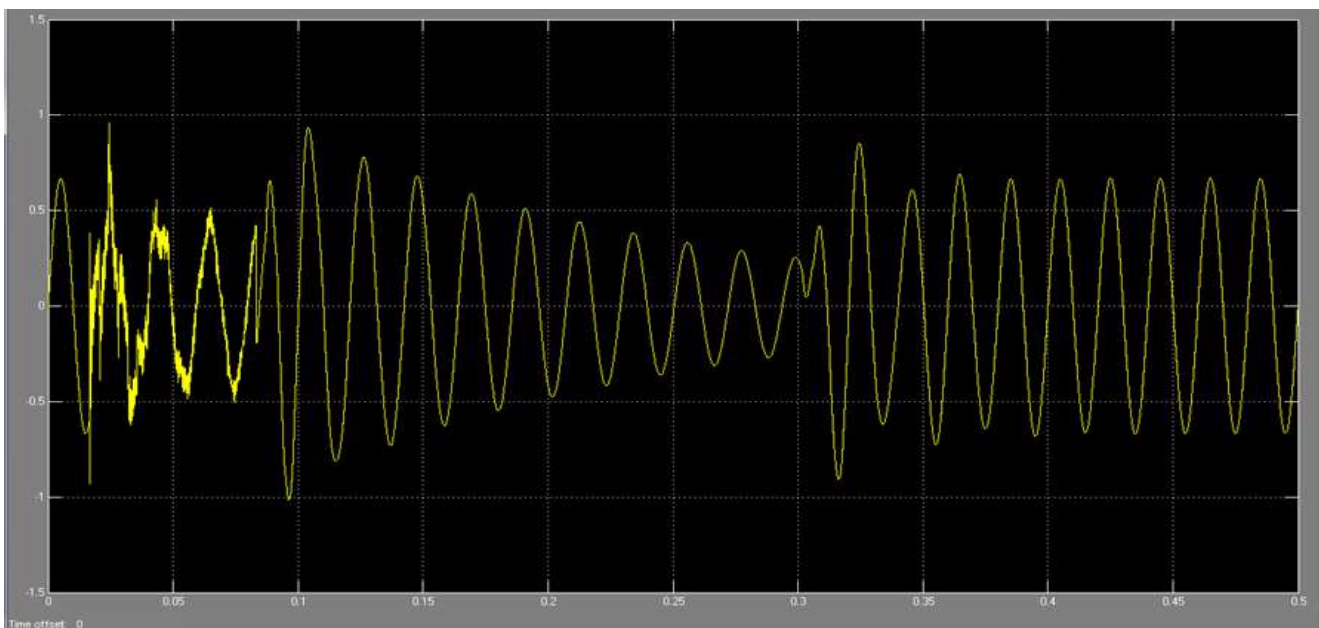

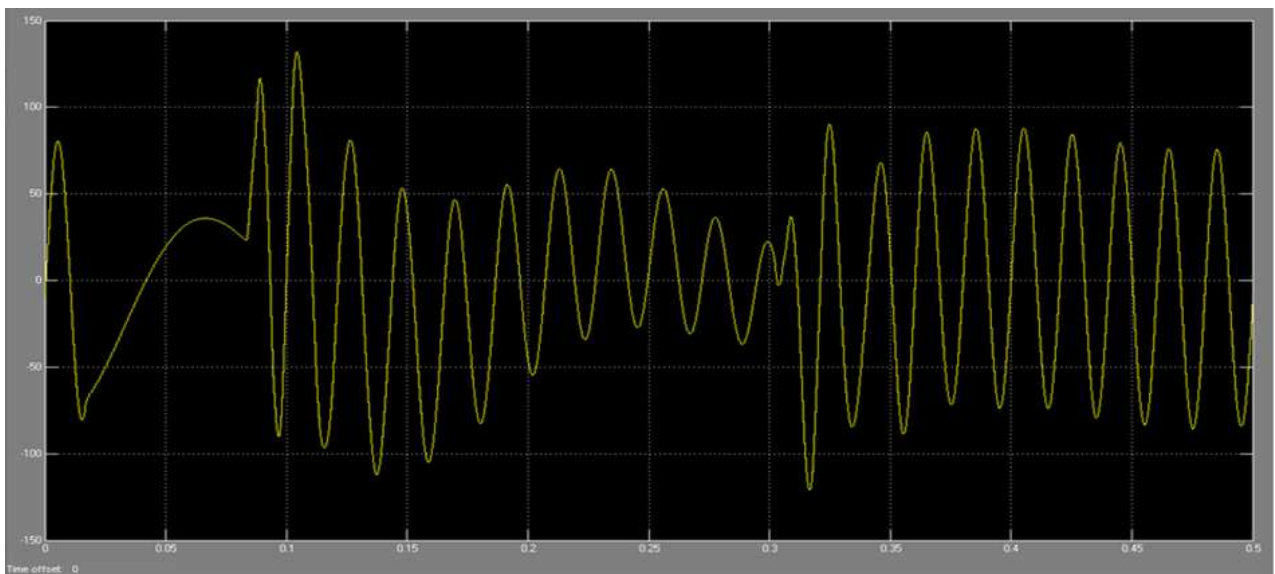Figure 9. Model for the line with one CCS and disturbance

3.4. Signal 1

In this case the breaker device was initially closed, an opening command was given at t = 5 cycles and then ordered to close again at t = 15 cycles. When the system was switched off, a spike current of about 10 times normal system current and about 8 times normal system current when switched on
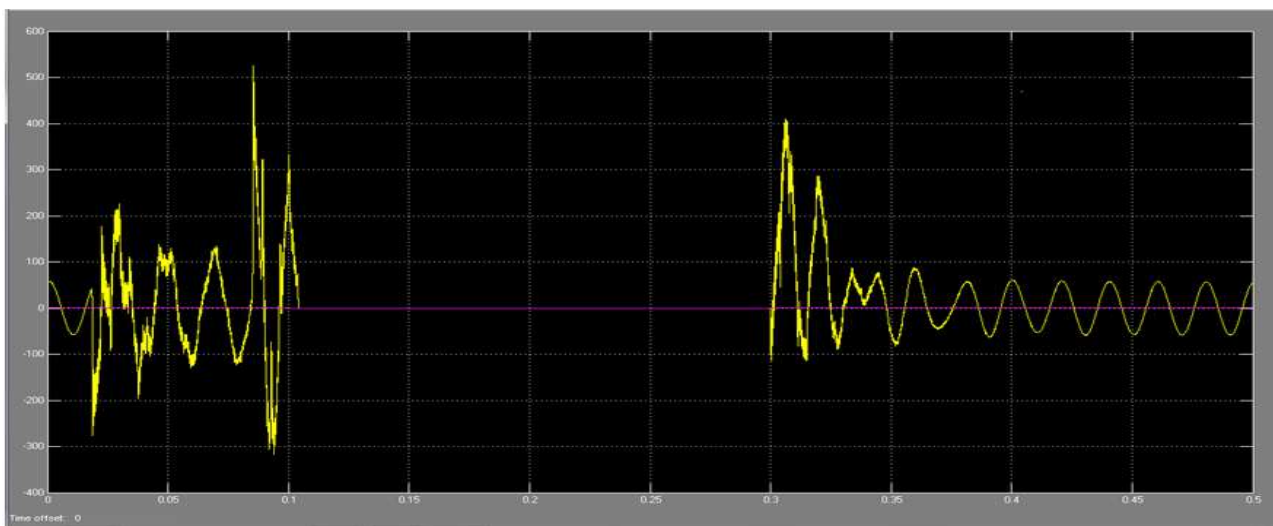
was observed see Figure 10(c).Additionally, a voltage overshot of about 1.3 time's normal tap-off voltage when the system was switched on or off was also observed. Further, the effect of switching resonance was clearly depicted on the system current and tap of voltage waveforms. Load current and load voltage waveform were observed to be in phase.
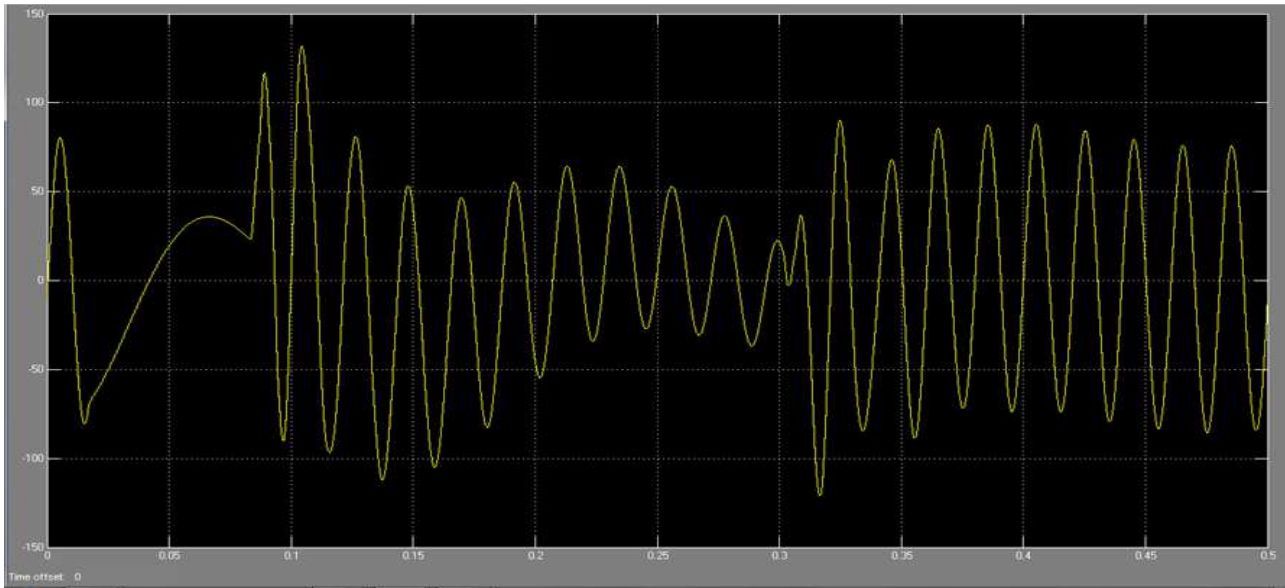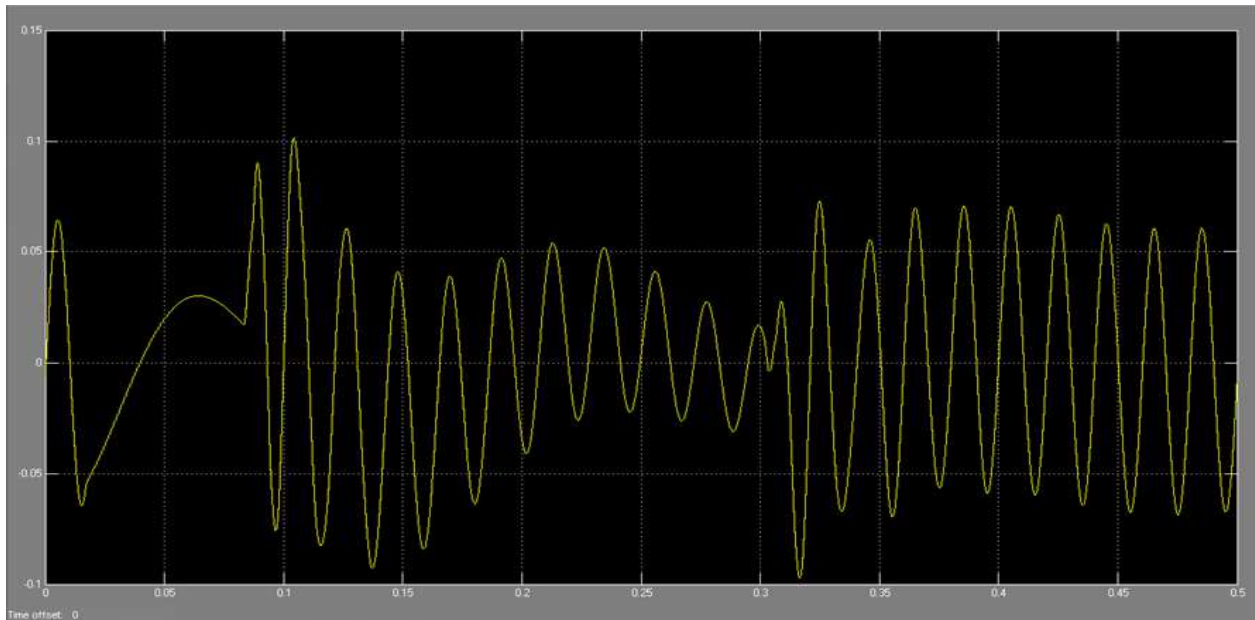
Tap-off Voltage Waveform (Scope 1)

Divider Voltage Waveform (Scope 2)

System current waveform (scope3)

(d) Load current waveform (scope 4)

(e) Load voltage waveform (scope 5)

Figure 10. Waveforms for Signal 1 Injection

4. Loadability Tests

The loadability test was carried out to determine the optimum apparent power that can be supported before the voltage begins to collapse. The tests were carried out for six different demand levels. For each test, real power demand P_L was fixed and reactive power demand Q_L varied and operated at different load power factor between 0.2 lagging to unity. Simulation results were tabulated. The desired maximum voltage at the load terminal was ± 6% of 33kV (from 31.02 kV to 34.98 kV). The tests were done at variable power factor using series R-L load model. Simulations of the

CCS system were carried out using the model circuit of Figure 12. Where;

Scope 1	U_1 - (kV) represents system tap-off voltage.
Scope 2	U_2 - (kV) represent capacitor banks voltage divider
Scope 3	U_3 - (kV) - represent load terminal voltage
Scope 4	I_1 - (A) represent system current.
Scope 5	I_2 - (A) represent current flowing at the capacitor bank divider
Scope 6	I_3 - (A) represent load current
	Q_L (MVA$_R$) - represent varied reactive power of the load

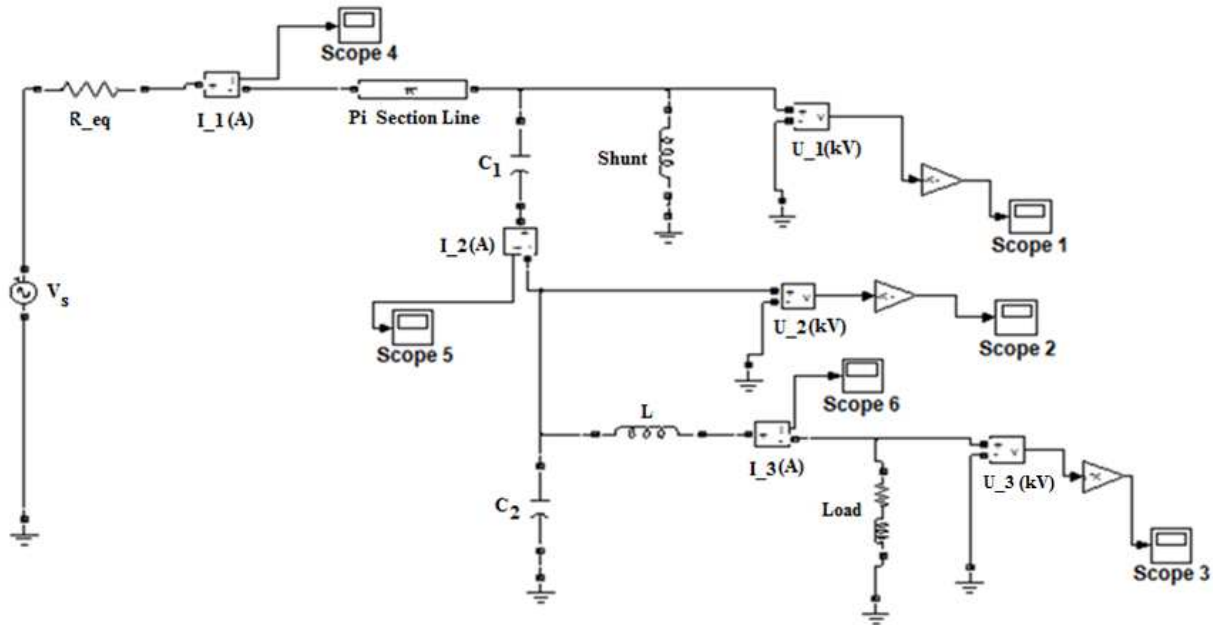Figure 12; show the loadability test graph for the six different demand levels.

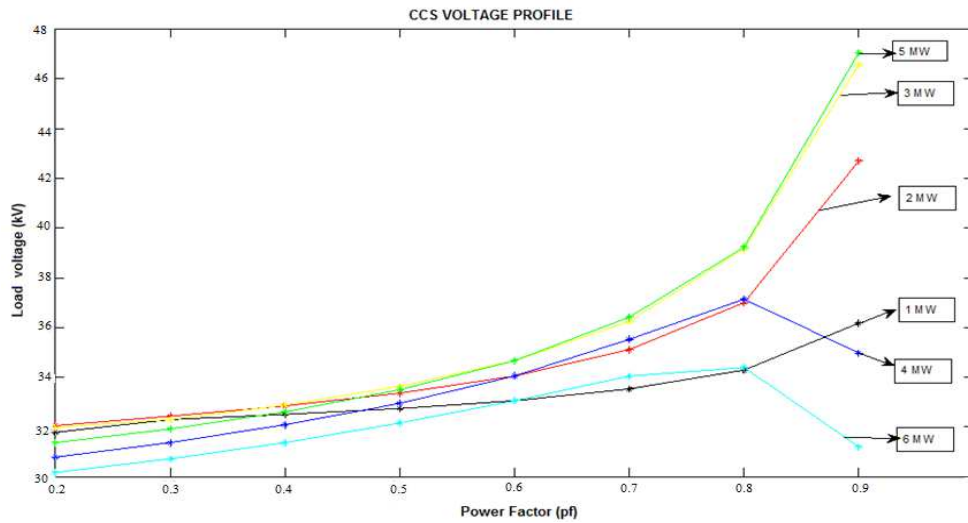

Figure 11. *CCS loadability test model*

Figure 12. *Voltage profile for loadability test*

Simulation results clearly showed that CCS system can be operated within allowable voltage regulation if a load of 1MW at 0.5 to 0.8 power factor was connected at the load terminal. The load current at these power factors ranged between 35.28A to 21.05A. It is worth noting that the 6MW load gave a good voltage profile between 0.5 and 0.8 power factors, but the load currents were quite high i.e. between 215.56A and 125.94A. For the other load demand scenarios, i.e. 2MW, 3MW, 4MW and 5MWthe system could operate between 0.2 and 0.6 power factor which would result to very high currents being drawn from the supply.

4.1. Shunt Compensation Using CCS

Compensation test was carried out using a similar diagram

of Figure 11, shown above. The shunt reactor was modeled by varying values corresponding to the active and reactive power specified in the simulation design. The value of C_1 and C_2 were maintained as derived in section two. Additionally, in this scenario, it was worth noting that compensation meant with a loaded CCS and un-compensation without CCS. The simulation results showed that CCS model improved the line voltage profile as seen from the analysis given in Figure 13 below. Three load scenarios were simulated i.e. 40, 70 and 125MW. These loadings were based on; when the transmission line is lightly, moderately and maximum loaded respectively. (Remember 125MW is the maximum loading of this line). In all the three scenarios it was observed that the compensated system showed a higher voltage than the

uncompensated. In this case, the line worked better at 40MW compensated load i.e. it operated within the ± 6 % of 127kV. The 70MW and 125MW load gave a lower voltage profile when compensated or uncompensated. Therefore, CCS helps in mitigating line losses in a loaded line. Conversely, CCS model may be installed on a heavily loaded line to improve the line compensation. When the line is lightly loaded, CCS may increase the voltage profile.
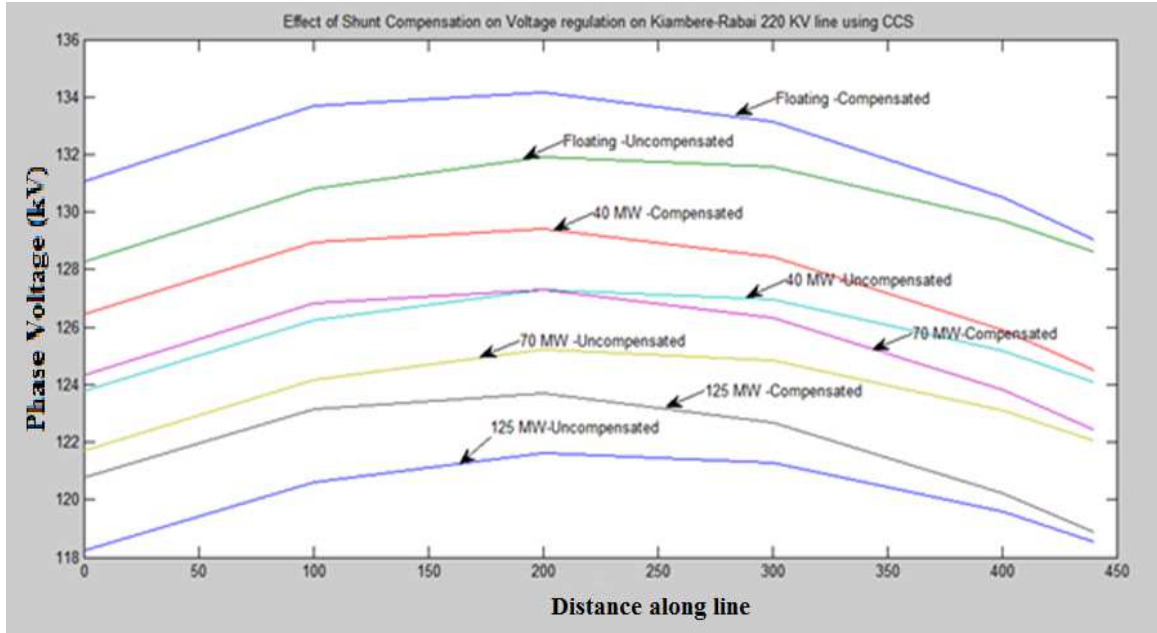

Figure 13. *CCS voltage profile for compensated and uncompensated line*

5. Penetration Level of CCS in Power Network

As explained earlier, connecting CCS units to a transmission power network will result to a change in the voltage profile. With the increase of CCS, it may be difficult to keep the voltage on the load side feeders within the allowable range in all situations. This will limit the amount of CCS that can be connected in a network [13, 14]. The main goal of this research project was to determine the maximum (with respect to the voltage change they cause) allowable penetration level of CCS units in a power network without violating the steady state voltage limit of the system. This section investigates how many CCS units can be allowed to penetrate the network when the voltage change caused by the CCS units is to stay below a certain limit. The CCS in this case is assumed to produce as much reactive power as possible to limit the voltage increase they cause. The maximum allowable penetration will be determined when the CCS units use maximum possible reactive power to compensate the voltage change they cause [15].The violation of the voltage limit is most likely to occur in high generation situations. In that case the CCS operates at or close to its nominal power and reactive power capability is limited. Similarly, the first way to increase the maximum penetration level of CCS is to use the CCS units to absorb reactive power from the grid.In this way the CCS unit can compensate (a part of) the voltage change it causes. The maximum compensation that can be achieved is limited by the maximum current of the CCS. However the maximum amount of reactive power that can be consumed is given by;

$$Q_{CCS.max} = \sqrt{(V_{CCS}I_{CCS.max})^2 - P_{CCS}^2} \qquad (19)$$

With Maximal CCS current defined as:

$$I_{CCS.max} = \frac{S_{dg} + S_S}{V_{CCS}} \qquad (20)$$

Where; S_{dg} is the apparent power from the DG
S_s is the power absorbed by the CCS
And V_{CCS} is the CCS voltage.

The active power that is supplied to the grid will result in an increase in Vccs due to the voltage drop across the impedance. Since, P_{CCS} is independent of V_{CCS}, this results in a decrease of the active current ($P_{CCS} = V_{CCS}I_{CCS} \cos\phi$) and thus an increase of the reactive power margin. In this way the CCS unit can undo part of the voltage increase caused by its active power. First, only the margin obtained in this way will be used and the maximum penetration level determined. The voltage change caused by the CCS units' active and reactive power can be calculated from;

$$V_{CCS} = V_S + Z_{SC}\frac{S_{dg}}{V_{dg}} \qquad (21)$$

The maximum number of installed CCS unit power ($P_{CCS.max}$) for a particular limit can be calculated by solving equation (19) to (21) iteratively.

5.1. Validation Test Using Voltage Sensitivities Analysis

The main factor that may limit the penetration level of CCS in a typical transmission system is the steady state voltage change. The maximum amount of reactive power supplied by CCS into the power network without causing voltage violation can be determined by using repetitive power flow studies as mentioned earlier.

In this research project the proposed method for estimating maximum allowable power injection into the network is based on voltage sensitivities related to active and reactive power injections [13, 14].The sensitivities are obtained from the load Jacobian matrix, which can be determined from the linearized power system model for a given base case (V^0, θ^0) as,

$$\begin{bmatrix} \Delta P \\ \Delta Q \end{bmatrix} = \begin{bmatrix} J_{P\theta} J_{PV} \\ J_{Q\theta} J_{QV} \end{bmatrix} \begin{bmatrix} \Delta\theta \\ \Delta V \end{bmatrix} \qquad (22)$$

Where, Δ denotes small variations in the variables. The elements of Jacobian matrix (J) represent the sensitivity among the power variations (ΔP, ΔQ) and voltage variation (ΔV, $\Delta\theta$) on the line.

In this work the Jacobian matrix (J) is represented by;

$$J = \begin{bmatrix} J_{P\theta} J_{PV} \\ J_{Q\theta} J_{QV} \end{bmatrix} \qquad (23)$$

5.2. V-P Sensitivity

Supposing that $\Delta Q = 0$ and $J_{Q\theta}^{-1}$ is non-singular, theSlack Bus – PV Bus Conversion equation can be rewritten as

$$\Delta P = (J_{PV} - J_{P\theta} J_{Q\theta}^{-1} J_{QV})\Delta V = J_{RPV}\Delta V \qquad (24)$$

And

$$\Delta V = J_{RPV}^{-1}\Delta P \qquad (25)$$

Where J_{RPV} is a reduced Jacobian matrix, which gives the voltage magnitude variations due to active power injection variations. The inverse of $J_{Q\theta}$ matrix is feasible only if all buses are modeled as PQ buses, guaranteeing that $J_{Q\theta}$ is a square matrix. This situation only occurs in distribution systems, where the slack bus is the only bus that keeps a varying voltage magnitude [14, 16].This is analogous to the CCS system where $V_{th}= V_0$ (See Figure 2) and should be maintained at a varying value. In addition, DG plants are usually modeled as PQ buses since they do contribute to the voltage control of the system [16].Similarly, when the CCS is modeled as Q instead of X_c, it can also contribute to voltage control. In our case, matrix J_{PV} can be used directly in order to indicate which buses of the system will be more or less affected by the installation of a CCS unit. However, matrix J_{PV} by itself does not give sufficient information about the sensitivities because the other matrices $J_{P\theta}, J_{Q\theta}$ and J_{QV} are

neglected.On the other hand matrix J_{RPV} is obtained without any approximation with respect to the characteristics of the system, since the relationship among variables V, θ P and Q are preserved. Equation 24 can be used to estimate the impact of multiple CCS system by representing (ΔP) as a diagonal matrix, with one entry of active power component injection for each CCS unit.In this case each column of ΔV will represent the impact of one CCS on the system voltage profile. The disadvantage of equation 24, however, is that only unity power factor CCS system can be considered, but in this research project a power factor of 0.2 to unity is considered. This draw back can be solved by using the V-Q sensitivity as explained.Analogous to V-P sensitivities, V-Q sensitivities can be determined by assuming $\Delta P = 0$ in theSlack Bus – PV Bus Conversion equation, resulting in

$$\Delta Q = (J_{QV} - J_{Q\theta} J_{P\theta}^{-1} J_{PV})\Delta V = J_{RQV}\Delta V \qquad (26)$$

And

$$\Delta V = J_{RQV}^{-1}\Delta Q \qquad (27)$$

Where J_{RQV} is a reduced Jacobian matrix, which states the voltage magnitude variations with relation to the reactive power variations.Equation 26, allows the estimation of the impact of CCS systems with different power factor on the system voltage profile. Again ΔQ can be organized as a diagonal matrix, whose elements would represent the absorption or the injection of reactive power of each individual CCS unit.The information obtained from these two sensitivities matrices (J_{RPV} and J_{RQV}) permits the estimation of voltage variations due to the installation of one or a group of CCS units with any desired power factor. By considering P_{CCS} as a diagonal matrix whose elements represent the active power injection of each CCS unit and Q_{CCS} as a diagonal matrix whose elements represents reactive power injection/absorption into the network, the voltage profile due to these additional CCS units can be estimated respectively, as

$$\Delta V_{(P_{CCS})} = J_{RPV}^{-1} P_{CCS} \text{ and } \Delta V_{(QCCS)} = J_{RQV}^{-1} Q_{CCS} \qquad (28)$$

Where $\Delta V_{(P_{CCS})}$ and $\Delta V_{(QCCS)}$ are, respective matrices that reflect the voltage profile deviation due to new active and reactive power injections of the CCS units assuming their installation at any distance on the network with respect to the base case. If just one CCS unit is considered, matrices ΔV will provide just a non-null column for each CCS, which should be summed in order to build up the new system voltage profile. Therefore, the estimated voltage profile after installation of one or a group of CCS units can be analytically expressed by;

$$V = V^0 + \Delta V_{(Pccs)} + \Delta V_{(Q_{CCS})} \qquad (29)$$

Where, V^0 is the voltage profile for base case. The reactive power impact on the voltage profile can be negative or

positive depending on the CCS power factor. The capacitive power factor leads to a voltage rise and inductive power factor to a voltage drop.Equation 29 allows one to estimate the voltage profile when the CCS at every possible distance of the power network, with any lead or lag power factor and any specified voltage level. The simultaneous usage of V-P and V-Q sensitivities to determine the voltage profile variation due to the installation of CCS units can be done through validation studies for different scenarios. These sensitivities can also be used for estimating the maximum allowable power injection

of a CCS unit.The usage of V-P and V-Q sensitivities to determine the impact of an additional CCS on the system voltage profile by using equation 29 is described in this section. In the following studies three 100kVA, CCSs were added to the 30 bus IEEE test system on buses 8, 22 and 28 as shown in Figure 15. This system replicates the Kenyan 132/22kV grid system. The CCS at bus 8 operated at 0.95 inductive power factors, the CCS at bus 28 at unity power factor and the CCS at bus 22 at 0.95 capacitive power factors.
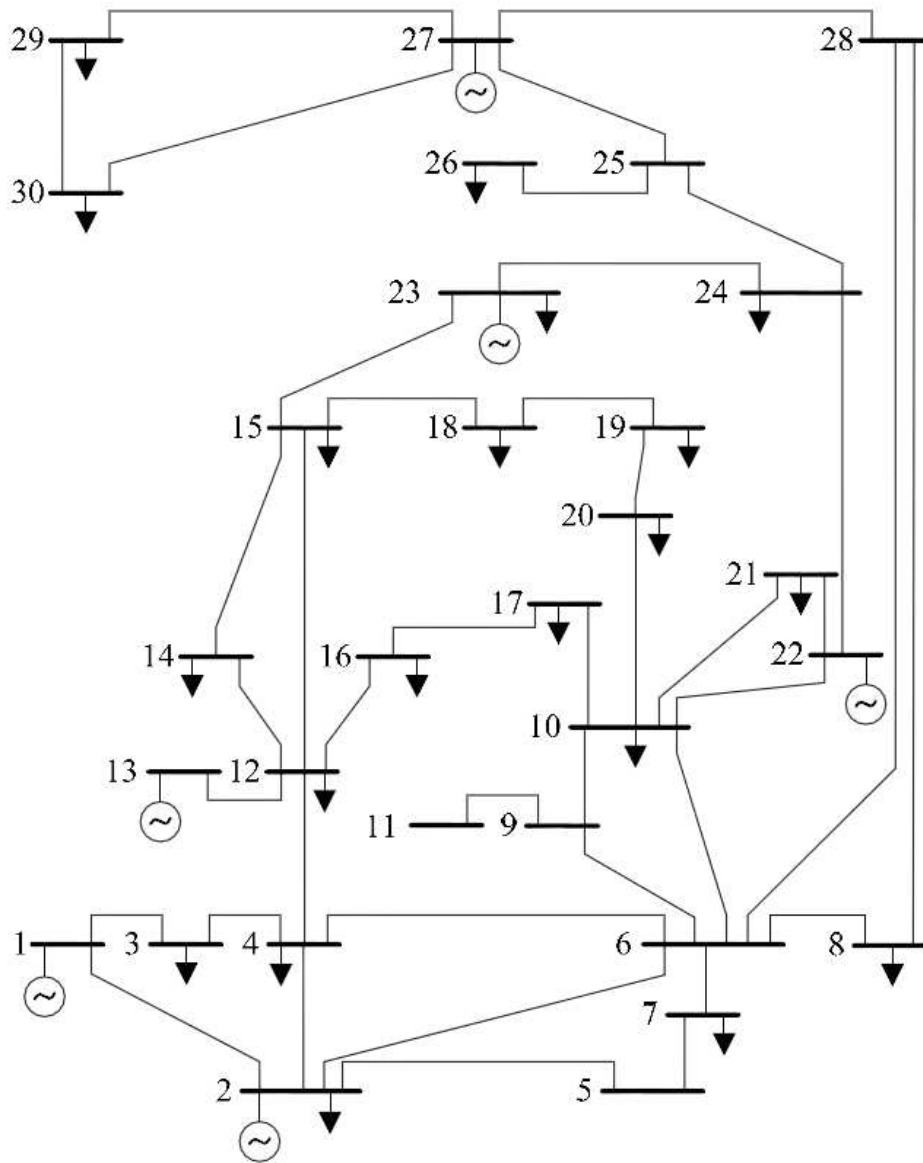

Figure 14. Single line diagram of the IEEE 30-bus test System

Figure 15, presents the voltage profile for the base case and the estimated voltage profile with the installation of one, two and three CCS, respectively, by using equation 29. The first CCS installed at bus 28 causes significant voltage rise even when operating at unity power factor. The buses on the main feeder are the most impacted, whereas the remaining buses suffer smaller voltage rise. The second CCS installed at bus 8, has little impact on the system voltage profile. Due to the fact

that it operates at an inductive power factor mode, hence, assist in balancing the reactive power of the line. The installation of a third CCS leads to voltage violations at the vicinity of bus 28, due to the combined effect of the two CCS. The CCS, installed at bus 22, drastically affects the whole voltage profile, since it injects simultaneous active and reactive power into the system. The combined impact of three CCS leads to severe voltage violation. This mainly takes place

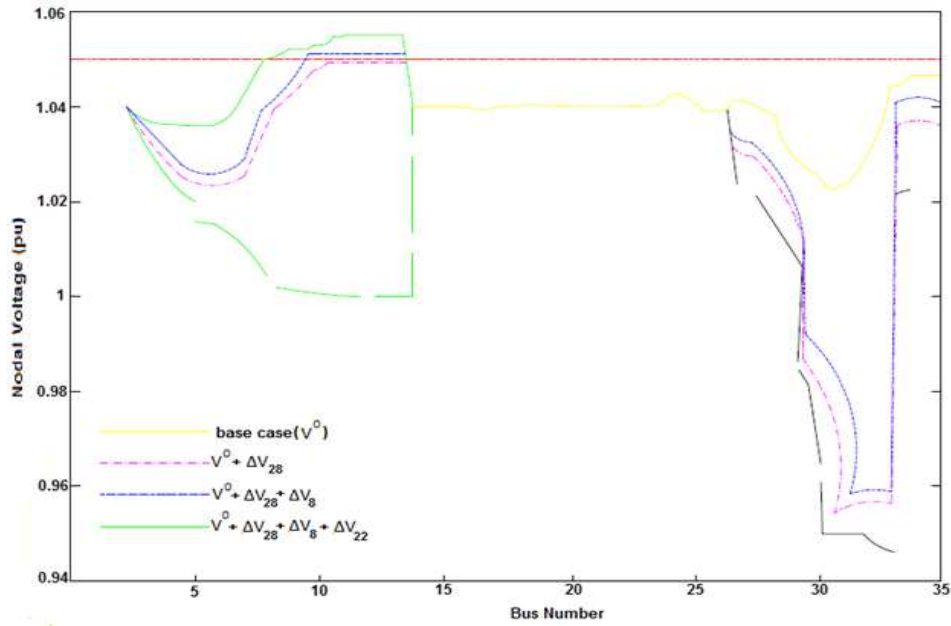at the end of the main feeders (16-28).

Figure 15. *Voltage profiles with CCS units at buses 8, 22, and 28.*

To justify why linearized equation 29 can be used, one CCS unit is considered to have been installed in bus 28 of the test network. Figure 16, illustrate the voltage behavior of bus 28.when the active power injection of the CCS is incremented by 1kW – steps until the superior voltage limit is reached. For each step a load flow is solved and then the graphic is plotted in Matlab software environment. The analysis considers three different power factor operation (pf = 0.9 inductive, pf = 1.0 and pf = 0.9 capacitive) and the maximum demand scenario. The linear behavior of the nodal voltage can be observed.

Indeed, the slopes of these lines are approximately equal to the sensitivity coefficients of J_{PQ} which are also shown in Figure 16. These results explain why the maximum capacity of CCS can be estimated by using voltage sensitivity analysis which is linearized equations. The behavior of CCS systems within narrow voltage variation is close to linear. Figure 16, reveals that, as expected, the capacitive operating mode presents a higher sensitivity coefficient than that of the other operating modes. Therefore, the amount of power injected for this operating mode is the lowest for the three analyzed cases.
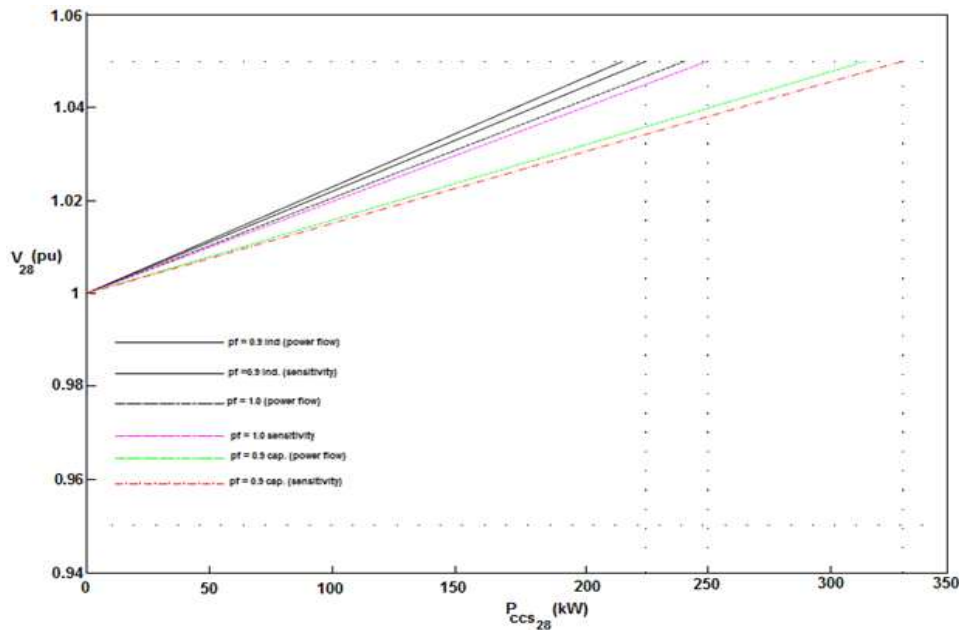

Figure 16. *Maximum Allowable Power of Bus 28*

In order to further validate the estimation of the system   voltage profile with the addition of another CCS by using

equation 29. A CCS unit of 100kW was installed at bus 11. The maximum demand scenario was considered and two different value of power factor were analyzed. The base case voltage profile (without any CCS unit) and the new voltage profile after the addition of the CCS are illustrated in Figure 17, This reveals that the results provided by the voltage sensitivity based methodology are very close to those obtained by use of successive load flow solutions. The capacitive operating mode case presents the largest voltage variation. Consequently, the major error is related to this case.
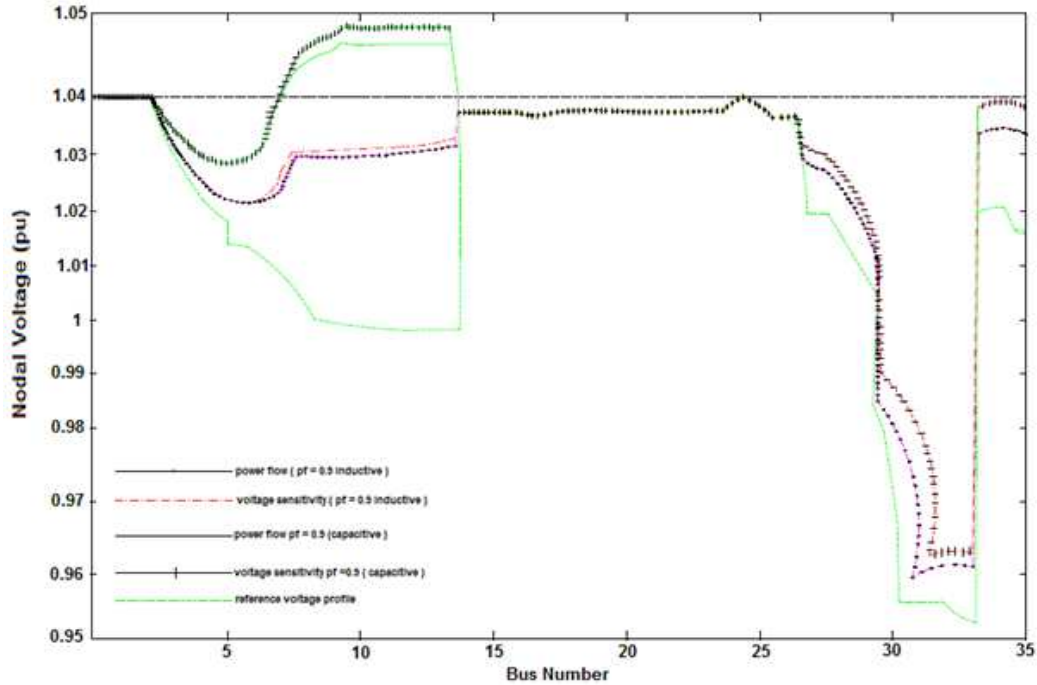

Figure 17. *Voltage profile for different power factors for ccs unit*

Figure 18, presents the evolution of the error between the estimated and compared voltage magnitude of bus 11 as a function of the active power injected by the CCS. Although, the error increases when the power is incremented, the maximum error is within an acceptable range for a linear method (lower than 0.2%).
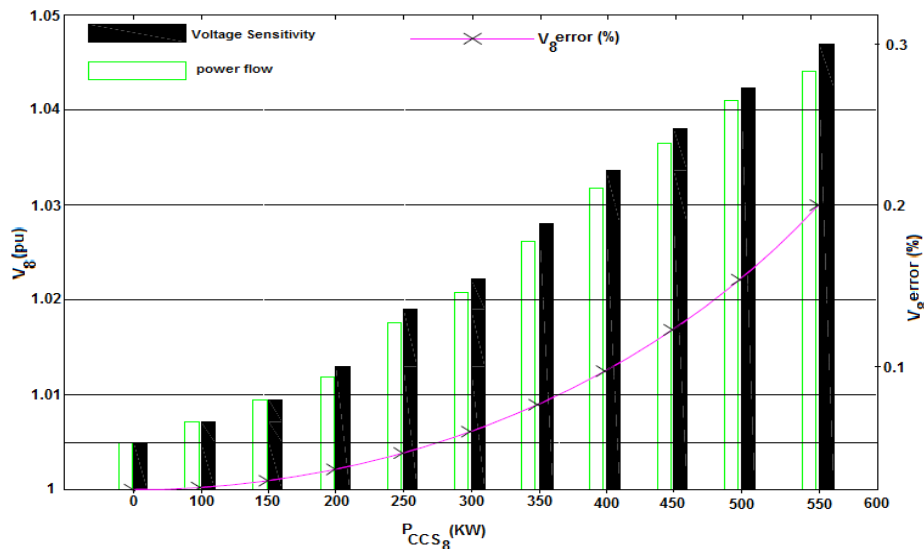

Figure 18. *Assessment of voltage sensitivity.*

6. Analysis of Results

The steady state simulation results of CCS system showed that the tap-off voltage on the transmission line increased by 20.73% during light load period and 5.087% during heavy load periods with respect to the supply. In addition, there was a decrease of the terminal load voltage at light and heavy load of about 0.04% and 13.33% respectively. The transient state simulation without the FSC circuit was carried out and different range of signals applied. During signals 1 to 4 the

system was switched off and on, a spike current of about 8 to 10 time's normal system current was observed. Furthermore, a voltage overshot of about 1.3 to 1.5 time's normal tap-off voltage when the system was switched on or off was also noted. In addition, the effect of Ferro-resonance was experienced on the divider voltage, load current and load voltage waveform. The loadability tests were also done at variable power factor using series R-L load model. Simulations of the CCS system were carried out in six different levels of demand. For each test real power demand (P_L) was fixed and reactive power demand (Q_L) varied to operate at different load power factor between 0.2 lagging to unity factor. The tests took into consideration the required load terminal voltage and the tap-off voltage constraints. Simulation results showed that the designed CCS system can be operated within allowable voltage regulation if a load of up to 1MW at 0.5 to 0.8 power factor was connected. Shunt compensation results showed that, the CCS helps in mitigating line losses in a loaded line. Conversely, CCS model may be installed on a heavily loaded line to improve the line compensation. When the line is lightly loaded, CCS may increase the line voltage profile. Various simulation studies were performed for different topologies of CCS design parameters. It was observed that penetration of a single CCS on the Rabai- Kiambere line caused increased Ferro-resonance resulting to the voltage waveform distortion towards the end of the transmission line. On switching, this distortion of impulses lasting about 3 to 6 cycles cumulatively may cause insulation failure of electrical equipment such as transformers connected to the line. In other words, Ferro-resonance problems persisted regardless of position of a single CCS along the line.Subsequently, penetration of two CCS of similar values as that of the single CCS penetration provided much improved voltage profile characteristics for both transmission line and the load output voltage from the sub-stations. The switching resonance effect was limited to less than two cycles. However, with additional penetration of an extra CCS of similar value as the first two, a smaller input capacitor was required, that may put a ceiling on what is possible to manufacture. Meaning, this would introduce standardization problems. Conversely, it was established that the CCS could be placed anywhere along the line. This meant that the maximum penetration point was not a function of the penetration level. Moreover, it was also proved through simulations at different distances on the line that penetration of the CCS per phase was dependent on the line parameters, the value of the CCS units installed and the loadability of the CCS. The requirement was to have the correct balance of all these parameters that could be accommodated without violating the maximum steady state voltage on the MV and HV side of the system. It was further observed that fast operating switchgears (operating in less than 1sec) are required for isolating faults on the low voltage network. This is to ensure a reduced voltage rise on the voltage divider for the capacitors protection.In this paper, an analytical methodology based on voltage sensitivity was used to directly estimate the maximum allowable power that a CCS can inject into the system without causing steady state voltage violations and assuming no substantial changes in system structure.

The results obtained by the proposed method were compared with those provided by repetitive power flow solutions in section three. The accuracy of the proposed method was shown to be adequate. It is important to emphasize that, although the proposed method had presented good performance, this is an approximated approach due to linearization of the system model. Further, it is important to call to attention that other technical aspects have to be analyzed when determining the maximum allowable CCS units in the system such as protection system and active power loses which cannot be addressed by the proposed method. Thus this method should be used only during preliminary investigation stages. The next chapter presents a case study of Auxiliary Service Voltage Transformers (ASVTs) in power networks.

7. Conclusion

The paper presented the implication of the un-conventional CCS technology for planning Rural Electrification in Kenya. It has highlighted the different aspects of this technology that makes it suitable for rural electrification planning in Kenya. It is evident that application of CCS has great potential for cost reduction. Therefore, a new outlook or approach in planning of Rural Electrification in Kenya is required. Consequently, system studies applying extensive modeling and simulation were necessary for a better understanding of the CCS technology and their adoptability in Kenya. This was done in order to maximize the benefit of these technologies to the rural consumers and also the overall power system stability. To enhance full operation and planning of current active transmission and distribution systems, an extensive study on penetration level optimization of the CCS technology on an existing power network in Kenya has been carried out on this paper. The expected results for this study were positive and valid. Consequently, they have quite a large implication for rural electrification in many developing countries especially in Africa.

Acknowledgements

References

[1]   Bolduc, L., Bouchard, and Beaulieu, G., "Capacitor divider substation," IEEE Trans. Power Delivery, Vol. 12 No. 3, pp. 1202-1209, July 1997.

[2]   Barnes D.F and Foley G. (2004): Rural Electrification in the developing world: A Summary of successful programs.Joint UNDP/World Bank Energy Sector Management Assistance Program (ESMAP) World Bank, Washington DC.

[3] Gaunt C.T (2005):HV SWER and Single phase systems CIGRE SC-C6 working group (Coll 2005) ...IWD Topic E2.

[4] Zomers A.N. (2003):The Challenges of rural electrification. Energy for sustainable development Vol VII No 1 (2003).

[5] Barnes D.F, (2007): The challenge of Rural Electrification: Strategies for developing countries. (Vol 1 pp1-18) Washington DC: Resource for the future.

[6] Saulo, M.J., Gaunt C.T., and Mbogho, M.S., (2012): Optimum Penetration level of un-conventional sub-station on a power transmission network. Proceedings of the 1st Applied Research Conference in Africa. 29th – 31st August 2012 Elmina, Ghana.

[7] Pasand, M.S., Aghazadeh, R., (2003).Capacitive Voltage Substations Ferro resonance Prevention using power electronics devices International conference on power system transients- IPST 2003 in New Orleans.

[8] Schilder, M., Britten A.C., Mathebula M.E., Singh A., (2005): Eskom Experience with On-Site Field Tests of Capacitive Coupled Substation. IEEE PES 2005 Conference and Exposition in Africa Durban, July 2005.

[9] Sarmiento, H.G., De la Rosa F., Carrillo, V., and Villar J., (1990): Solving Electric Energy Supply to Rural areas: The Capacitor Voltage Divider. IEEE Transaction on power delivery, Vol 5, No 1, January 1990.

[10] Raphalalani, T.V., Ijumba N.M., Jimoh, A.A., (2000): Capacitive Divider System for feeding a distribution network from an EHV line. Powercon 2000 Lusaka.

[11] Kothari, D.P., Nagrath, I.J., (2006): Modern Power System Analysis Mc Graw Hill, 2006.

[12] Kenya Power and Lightning Co.Ltd and ministry of Energy (KPLC), 2009 Update of Kenya's least cost power Development plan 2009-2029.

[13] Ayres, H.M., Freitas, W., De Almeida M. C., Da Silva, L.C.P., (2010): Methods for determining the Maximum Allowable Penetration Level of Distributed Generation without steady-state voltage violation   IET Generation, Transmission and Distribution 2010 Vol 4, pp495-508.

[14] Jinfu, C., Rongqi, F., Xianzhaong, D, Jingliana, C., (2006): Penetration level optimization for DG considering reliable action of relay protection device constraints. IEEE Transaction on Power Systems vol 17, No3 2006.

[15] Morren Johan, De Haan., and Sjoerd W.H., "Maximum Penetration level of Distributed generation without violating voltage limits".In Proc.2006 Power Engineering Society General Meeting7PP357

[16] Nan Jiang, JianrongGong.DeqiangGan "Computing the maximum Penetration level of Distributed Generators in Distribution network by taking into account   harmonic constraints"Automation of electric power system systems vol 31pp19-23 2007